

NOTES AND CORRESPONDENCE

Transient Diapycnal Mixing and the Meridional Overturning Circulation

WILLIAM R. BOOS, JEFFERY R. SCOTT, AND KERRY A. EMANUEL

Program in Atmospheres, Oceans, and Climate, Massachusetts Institute of Technology, Cambridge, Massachusetts

18 September 2002 and 18 June 2003

ABSTRACT

An idealized three-dimensional model of buoyancy-forced flow in a single hemisphere is used to investigate whether transient diapycnal mixing can sustain the meridional overturning circulation. In the annual mean, mixing transience had little effect on the meridional overturning. When mixing occurred on basin boundaries, the overturning strength was found to be insensitive to mixing transience. For mixing that was highly localized in space away from basin boundaries, oceanic meridional mass and heat transport decreased as mixing became more transient. The increased sensitivity in the highly localized case is likely due to the inhibition of surface heat flux into the thermocline. The dynamic response to transient mixing featured large-scale, internal oscillations that increased in amplitude with the transience of mixing but were confined to the Tropics and had little effect on the overturning cell through midlatitudes. These results indicate that transient diapycnal mixing, with a distribution suggestive of tropical cyclones, can effectively drive a meridional overturning.

1. Introduction

The mechanisms and distribution of diapycnal mixing are outstanding issues in physical oceanography. Their determination is relevant not only to understanding what drives the meridional overturning circulation (MOC), which plays a critical role in our climate system, but also to forecasting the dispersal of ocean tracers such as dissolved carbon and biological nutrients. Munk (1966; see also Munk and Wunsch 1998; Ganachaud and Wunsch 2000) inferred that a global average vertical diffusivity on the order of $10^{-4} \text{ m}^2 \text{ s}^{-1}$ was necessary to maintain the abyssal stratification against global upwelling. Estimates from microstructure data suggest considerably lower diffusivities of order $10^{-5} \text{ m}^2 \text{ s}^{-1}$ in parts of the abyss and in the thermocline, implying that mixing is strongly localized (Toole et al. 1994; Kunze and Sanford 1996; Moum and Osborn 1986).

One such place where there is both observational and theoretical support for enhanced mixing is in the deep ocean. Abyssal measurements near rough bathymetry have yielded local diffusivities as large as $10^{-1} \text{ m}^2 \text{ s}^{-1}$ (Toole et al. 1997; Polzin et al. 1997; Ferron et al. 1998), suggesting that internal waves generated by flow over topography are a likely mechanism of diapycnal mixing. Modeling studies have also shown that flow over rough

bathymetry can generate considerable turbulent mixing (Legg 2004). Scott and Marotzke (2002, hereinafter SM02) used an idealized three-dimensional model of buoyancy-forced flow to investigate the sensitivity of the MOC to the location of diapycnal mixing. They found that while enhanced abyssal mixing did drive an active abyssal circulation, it did not generate additional flow through the thermocline, producing little change in the MOC's heat transport. Rather, their model results suggest that diapycnal mixing is needed in regions of strong stratification to support a vigorous MOC in the thermocline.

In light of the fact that tropical cyclones efficiently mix the upper ocean and that an estimate of the net ocean heating induced by cyclone mixing amounts to a substantial fraction of the poleward oceanic heat flux, Emanuel (2001) proposed tropical cyclones as an important mechanism of diapycnal mixing. Mixing induced by tropical cyclones would be highly transient, intense, spatially localized, and positioned in the upper ocean. Various studies have explored the sensitivity of the MOC to localized boundary mixing (Marotzke 1997; Samelson 1998; Marotzke and Klinger 2000; Scott 2000; SM02), seemingly with only minor impact on MOC dynamics as compared with spatially uniform mixing. Hasumi and Sugimotohara (1999) investigated the effects of enhanced mixing over topography in a global model. SM02 consider an extreme case of localized mixing, that is, in a single column of their ocean model. While the horizontal location of mixing has dynamical

Corresponding author address: William R. Boos, MIT, Rm. 54-1611, Cambridge, MA 02139.
E-mail: billboos@mit.edu

consequences, SM02 found that mixing at low latitudes was effective at generating a vigorous MOC, regardless of the zonal location. In contrast with these studies on spatially varying mixing, however, the sensitivity of the MOC to transience of diapycnal mixing seems completely unexplored.

This study aims to find whether highly transient diapycnal mixing can maintain a strong MOC. Using the idealized model of SM02, we expand upon their “single column” and “boundary” mixing results by examining the MOC response as mixing is made increasingly transient. One goal of this effort is to provide a concept feasibility test for tropical cyclones as a driving mechanism of the MOC. In more general terms, we seek to establish bounds on the characteristics of mixing that would effectively maintain the MOC.

The remainder of this note is devoted to exploring the numerical model, its results, and its implications. Section 2 describes the model configuration and the experiments that were conducted. Section 3 provides the results of these experiments, considering first the annual mean behavior, second the transient response to intra-annual changes in diapycnal mixing, and last the work done by diapycnal mixing. The last section discusses these results in the context of determining the driving mechanisms of the MOC, with special attention given to tropical cyclones.

2. Methods

a. Model description

The model used here is the same as that used in SM02 with minor modifications. The model is the Modular Ocean Model, beta version 2.0 (MOM 2), a z -coordinate, primitive equation, general circulation model developed by the Geophysical Fluid Dynamics Laboratory and documented in Pacanowski (1996).

The spatial domain extends from the equator to 64°N , is 60° wide with the western boundary at 0° longitude, and has a constant depth of 4500 m with no topography. The model was run at a spacing of 3.75° zonally by 4° meridionally, with 16 vertical levels varying in height from 50 m at the surface to 500 m at depth. Although SM02 performed most runs at the higher resolution of $1.875^{\circ} \times 2^{\circ} \times 30$ vertical levels, they noted that results differed little when the lower resolution was used. A representative subset of the experiments described below was conducted at this higher $1.875^{\circ} \times 2^{\circ}$ resolution as a test of numerical convergence. Runs conducted at different resolutions displayed only minor differences in overturning strengths, so that the higher-resolution runs support the results described below.

Integration was performed asynchronously with time steps of 24 h for tracers and 1 h for velocity and density. To confirm that the use of asynchronous integration did not considerably distort the transient response that is central to the results of this study, the run with the most

transient forcing was repeated with synchronous integration using a 1-h time step. Comparison revealed that, although the use of asynchronous integration distorted the detailed transient response of the circulation to some extent, the circulation in runs integrated both synchronously and asynchronously averaged to the same state over the course of 1 yr (see section 3 for more details).

In the surface layer, the model was restored to zonally uniform, time-invariant profiles of temperature and salinity that vary meridionally as the cosine of latitude, with peak-to-peak amplitudes of 27°C and 1.5, respectively. A restoring time constant of 30 days was used for all runs. A simple time-invariant, zonally uniform, idealized wind stress profile consisted of easterlies across the southern half of the domain and westerlies across the northern half (following Marotzke 1990). The rigid-lid approximation was employed at the ocean surface.

Diapycnal mixing was applied by changing the value of the vertical diffusivity κ . The pelagic diffusivity was simulated by using a minimum, background diffusivity of $10^{-5} \text{ m}^2 \text{ s}^{-1}$; higher diffusivities were used in grid cells for which mixing was desired. For reference, a run conducted with only the minimum background diffusivity produced an overturning of 2.7 Sv ($1 \text{ Sv} \equiv 10^6 \text{ m}^3 \text{ s}^{-1}$). The effect of mesoscale eddies was parameterized using the scheme of Redi (1982) and Gent and McWilliams (1990), with zero explicit horizontal diffusion.

b. Experiments

Two categories of runs conducted in SM02 were selected as the basis for this study: runs in which mixing was applied in all grid cells adjacent to a basin boundary and runs in which mixing was applied entirely in a single column of vertical grid cells away from boundaries in the subtropics. In the former case, mixing can be thought to be concentrated primarily along the equator (a boundary in our single-hemisphere “box”). In the latter case (“highly localized mixing”), the mixing column was centered at 10°N and 24.375°E . In reality, the mixing that results from tropical cyclones is not likely to be so acutely localized as our highly localized case (see section 4); we consider this case to be an extreme scenario to facilitate a dynamical understanding.

For each of these two categories, a set of runs was performed in which mixing was applied for 12 (the control case), 6, 3, 2, and 1 month of each year. The months in which mixing was applied were contiguous within each year, and κ was changed as a step function of time between the “off” value of $10^{-5} \text{ m}^2 \text{ s}^{-1}$ and the “on” value used for each particular run (Table 1), with no variation in the vertical direction. The boundary mixing run with no time variation (12 months per year of mixing) was made similar to experiment A of SM02 by using the same value of κ in boundary cells (the most noticeable difference being the inclusion of wind in this

TABLE 1. Vertical diffusivities of tracers used in each model run. The time- and area-weighted diffusivity for latitudes 0° – 36° N was held constant across all runs, neglecting the contribution from the pelagic diffusivity.

	Diffusivity during on state ($\times 10^{-4} \text{ m}^2 \text{ s}^{-1}$)
Boundary mixing	
12 months on, 0 off	5
6 months on, 0 off	10
3 months on, 9 off	20
2 months on, 10 off	30
1 month on, 11 off	60
Highly localized mixing	
12 months on, 0 off	160
6 months on, 6 off	320
3 months on, 9 off	640
2 months on, 10 off	960
1 month on, 11 off	1920

study). For the transient mixing runs, the time-weighted diffusivity of each boundary mixing run was held the same as in this control run. For runs with highly localized mixing, the diffusivities were set so that the area-weighted diffusivity was equal to that of latitudes from 0° to 36° N for the corresponding boundary mixing run (SM02 found that boundary mixing at latitudes greater than 36° N had little effect on the magnitude of the MOC). Thus, in all runs performed for this study, the area- and time-weighted diffusivity for latitudes 0° – 36° N was constant.

Each run was integrated from the respective steady state (i.e., with time-invariant mixing) until a new annual mean equilibrium was reached, as indicated by annual mean spatially averaged ocean–atmosphere heat exchange of $5 \times 10^{-3} \text{ W m}^{-2}$ or less and annual mean overturning within 0.1 Sv of its apparent final value. This required about 300 yr of simulation time.

3. Model results

a. Annual mean behavior

All boundary mixing runs displayed nearly identical annual mean overturning streamfunctions, with a weak decrease (about 4%) in the strength of overturning as mixing transience increased from the control to the most highly transient case. Figure 1 shows that the annual mean streamfunctions for the control case and the most transient case of boundary mixing exhibit only minor differences. For highly localized mixing, the inverse relationship between overturning strength and mixing transience was considerably stronger, with 25% less overturning for the most transient case than for the control. Figure 2 depicts the effect of increasing mixing transience on the spatial maximum of the annual mean overturning streamfunction.

The surface restoring timescale most likely causes the increased sensitivity of the MOC to transience in the case of highly localized mixing. When surface restoring

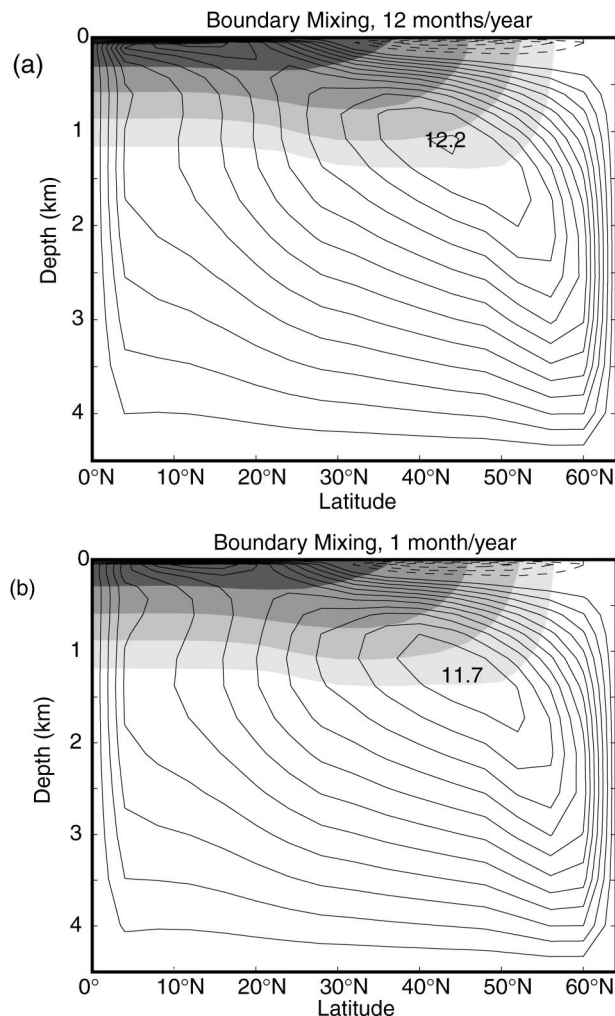


FIG. 1. Annual mean meridional overturning streamfunction (contours) and zonally averaged temperature (shading) for (a) time-invariant boundary mixing and (b) the most transient case of boundary mixing (all mixing during 1 month per year). Streamfunction contour interval is 1.0 Sv. Temperature contour intervals are 80%, 40%, 20%, 10%, and 5% of the approximate surface-to-bottom temperature differential of 27°C .

is effectively limited to a small area (i.e., where vigorous mixing is occurring), this process becomes rate limiting, resulting in a mixing-site SST that is 10° – 15°C lower than nearby grid cells. In more fundamental terms, the restoring time scale effectively limits how fast buoyancy can be pumped into the system through the surface boundary conditions. For time-invariant highly localized mixing, SM02 showed that decreasing the temperature restoring time scale from 30 to 2 days resulted in an increased overturning. We find that with increased mixing transience, this “bottleneck” is increasingly effective at limiting the diffusion of buoyancy into the thermocline. It is presumed that the use of more realistic atmosphere–ocean coupling and/or a faithful representation of small-scale horizontal motions in the ocean’s mixed layer would reduce this limitation, resulting in

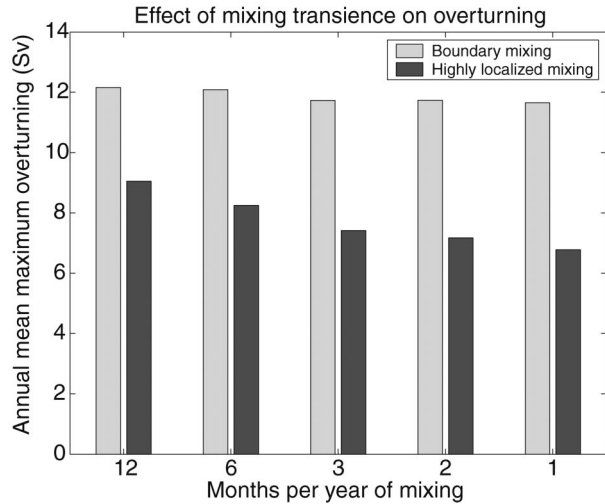


FIG. 2. Spatial maximum of the annual mean overturning streamfunction for all experiments.

less sensitivity to mixing transience. In the boundary mixing case, mixing is spread over a sufficiently large area so that any bottleneck is minimal, even in the case of transient mixing.

The net meridional oceanic heat flux behaved similarly to the total mass transport. Meridional oceanic heat flux was computed as an annual-mean, zonally averaged function of latitude (Fig. 3). The shape of the heat transport curve as a function of latitude does not vary significantly with mixing transience, at least at the spatial resolution used in this study.

b. Transient response

Figure 4 displays two instantaneous overturning streamfunctions (plotted from runs using synchronous

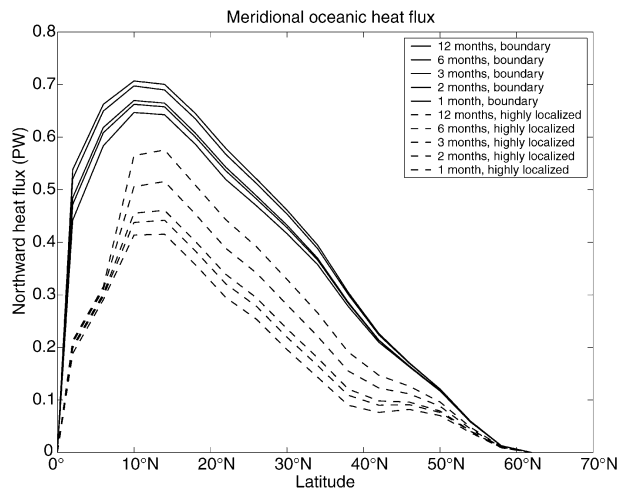


FIG. 3. Zonally averaged, annual-mean northward oceanic heat flux as a function of latitude for 1 yr at annual mean equilibrium. Curves follow the order given in the legend, from top to bottom.

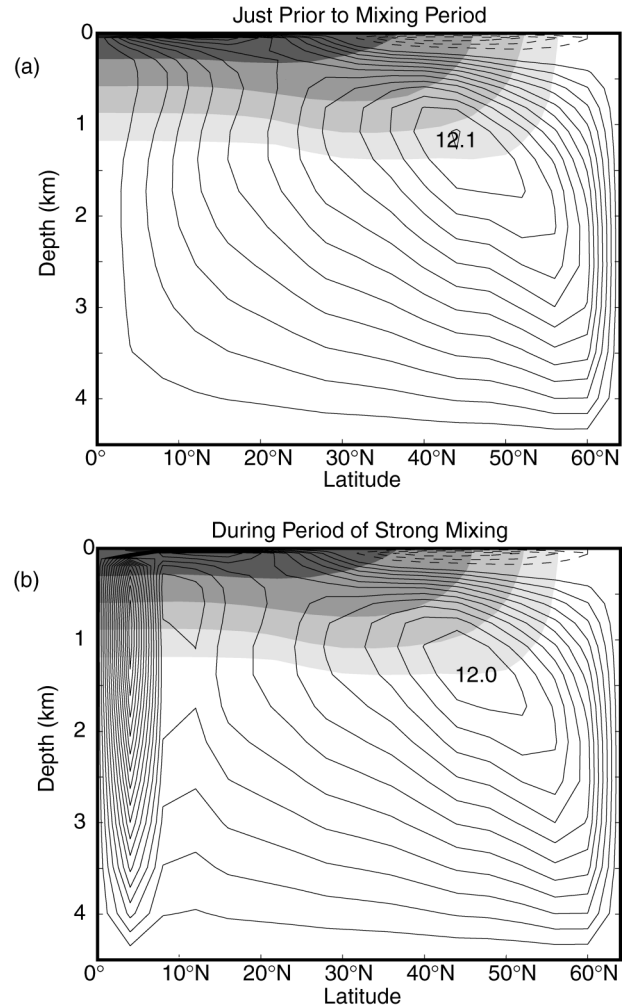


FIG. 4. Instantaneous overturning streamfunctions (contours) and zonally averaged temperature (shading) for the most transient case of boundary mixing (a) 2 days before the 1 month of mixing and (b) at the midpoint of the 1 month of mixing. Streamfunction contour interval is 1.0 Sv. Temperature contour intervals are 80%, 40%, 20%, 10%, and 5% of the approximate surface-to-bottom temperature differential of 27°C.

integration) for the most transient case of boundary mixing (the behavior in the highly localized transient run is qualitatively similar). The most notable features of these streamfunctions are the intense overturning cell in the southern 10° of the basin that exists when mixing is turned on and the robust overturning cell that occupies the majority of the basin and changes little as mixing is turned on and off. Figure 5 displays the time evolution of the midlatitude spatial maximum of the main overturning cell for the most transient cases of both boundary and highly localized mixing. The intense tropical overturning cell averages nearly to a state of no motion over the course of one year, contributing to the annual mean overturning only through a slight intensification of tropical upwelling.

The intense tropical overturning cell suggests ad-

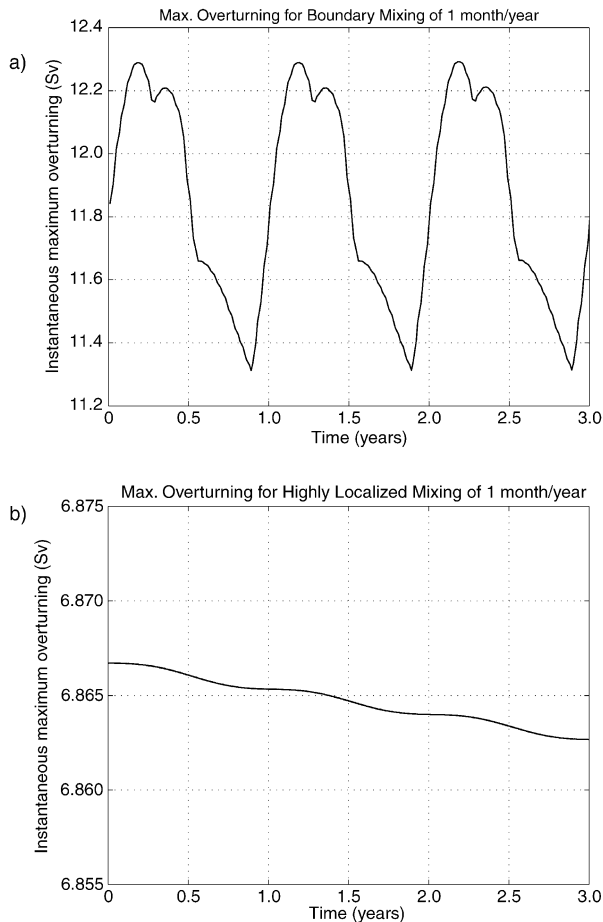


FIG. 5. Evolution of the spatial maximum of the midlatitude cell for the most transient case of (a) boundary mixing and (b) highly localized mixing. Note the change in vertical scale between plots. In both runs, mixing was applied for 1 month starting at 0.46 of each year. The downward trend in (b) is a residual drift toward equilibration of this run.

justment to changes in buoyancy forcing through large-scale internal waves. Changes in boundary mixing presumably excite boundary-trapped waves [either Kelvin waves or the boundary waves discussed in Killworth (1985) and Winton (1996)] as well as westward-propagating baroclinic Rossby waves. Highly localized mixing, being located away from boundaries, primarily excites Rossby waves. We expect that boundary waves, with characteristic timescales on the order of months, result in intra-annual fluctuations in the main overturning cell seen in the boundary mixing runs (Fig. 5a). Such intra-annual fluctuations are virtually absent in the case of highly localized mixing, which requires slower Rossby waves and/or advective processes to propagate the effect of transient mixing. It is interesting to note that in the most transient case of boundary mixing (Fig. 5a) the overturning peaks shortly before mixing is applied in each annual cycle and then decreases during and for several months after the period of mixing. The

dynamics underlying this behavior presumably involve the large-scale wave response, a detailed diagnosis of which is left for future work.

The principal difference between runs integrated synchronously and asynchronously was seen in the behavior of the tropical overturning cell, which reversed direction several times each year in a large-scale oscillation when asynchronous integration was used. However, this tropical cell had the same contribution to the annual mean overturning irrespective of the integration method. This result indicates that although the use of asynchronous integration distorted wave behavior in the model, it did not affect the annual mean results described above. Synchronous integration would need to be used in any future diagnosis of the detailed internal wave behavior.

c. Mixing energy

Were a constant energy source to supply mixing processes in the ocean, the total work done by mixing would remain fixed as the transience of mixing varied. However, in practice, prescribing a constant mixing power in ocean general circulation models adds complexity and requires additional ad hoc assumptions (Huang 1999), and therefore the de facto standard is to instead prescribe or parameterize vertical diffusivity. As such, the work done by mixing is a function of both the prescribed diffusivity and the resulting stratification. In this section we calculate the work done by mixing for our experimental runs.

Calculating a potential energy budget for an ocean model that uses a nonlinear equation of state in conjunction with the Boussinesq approximation is problematic: such models conserve volume without conserving mass, and so it is somewhat misleading to equate the quantity ρgz (where ρ is density and g is gravitational acceleration) with potential energy, because this quantity is not strictly conserved [see McDougall et al. (2002) for a more general discussion of conservation properties in Boussinesq ocean models]. Nevertheless, we have computed the power required for vertical mixing in our runs, on the presumption that errors related to the Boussinesq approximation do not obscure the more fundamental relationship between mixing transience and ocean energetics.

A useful expression for the power P expended in vertical mixing is derived by applying the chain rule to the Lagrangian derivative of in situ density, substituting the parameterized diffusivities for vertical mixing, and manipulating to obtain

$$P = gz \frac{\partial \rho}{\partial S} \bigg|_{\theta, z} \frac{\partial}{\partial z} \left(\kappa \frac{\partial S}{\partial z} \right) + gz \frac{\partial \rho}{\partial \theta} \bigg|_{S, z} \frac{\partial}{\partial z} \left(\kappa \frac{\partial \theta}{\partial z} \right), \quad (1)$$

where S is salinity and θ is potential temperature. The spatially integrated power expended in vertical mixing, time-averaged over 1 yr, was computed for each run using Eq. (1) and is displayed in Fig. 6. The turbulent

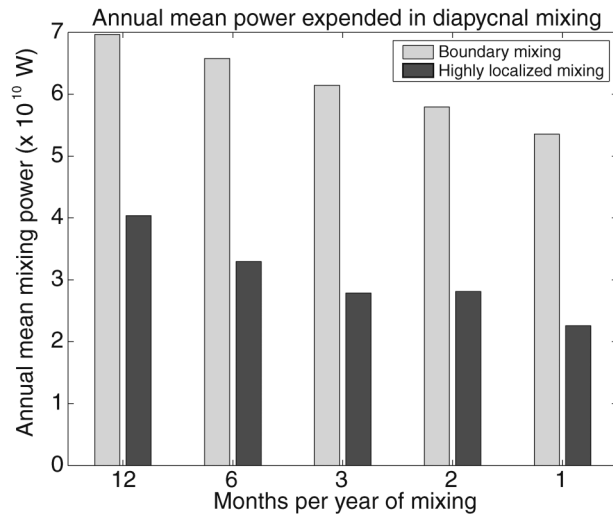


FIG. 6. Spatially integrated power expended in diapycnal mixing, time-averaged over 1 yr, for all experiments.

energy required to achieve this mixing power will be several times as great as these figures, given that only a fraction of the original input is converted into changes in the potential energy field. Estimating this fraction at 15% (Osborn 1980) yields a required turbulent input of about 0.25 and 0.5 TW for the highly localized and boundary mixing runs, respectively.

Several terawatts of power are believed to drive global ocean mixing, with roughly 1 TW coming from each of wind work on geostrophic ocean currents (Wunsch 1998) and tidal dissipation (Egbert and Ray 2001). Alford (2001) estimated an additional 0.3 TW flux from winds to near-inertial mixed layer motions between 50°N and 50°S. It is not obvious how these estimates should be compared with the model results, given that their spatial distributions may differ and that the model overturning and associated heat transport are sensitive to the spatial distribution of mixing (SM02). That is, some of the globally estimated mixing may result in density changes and flow not represented in the model. Nevertheless, after scaling to allow for the fact that the model results are for one-half of a single ocean basin, the required turbulent input computed for the model is of the same order of magnitude as the estimated total global power available for mixing.

The use of asynchronous integration had little effect on the results obtained for annual mean power; for the most transient case of boundary mixing, the results for a run integrated synchronously differed by less than 1% from results for a run integrated asynchronously. Although mixing power, annual mean overturning, and northward heat flux all decrease as mixing becomes more transient, mixing power decreases most significantly, implying that the MOC can be driven more efficiently by highly transient mixing. This result is surprising, although we cannot offer any explanation for this behavior. Further, it underscores our conclusion that

highly transient mixing can effectively drive a meridional overturning.

4. Discussion and conclusions

Climate models generally assume the distribution and intensity of ocean diapycnal mixing to be independent of the climate state. The existence of feedbacks between climate variables and diapycnal mixing could alter the equilibria attained in models and the sensitivity of climate to various forcings. Emanuel (2001) proposed tropical cyclones as a mechanism of wind-driven mixing that is sensitive to climate. To establish the role of tropical cyclones in a feedback between the climate state and the meridional overturning, it must be shown that the distribution or intensity of tropical cyclones varies as a function of some climate variable and that tropical cyclones induce ocean mixing that is capable of driving the MOC. The following discussion addresses these conditions. Note that we do not seek to establish tropical cyclones as phenomena responsible for all, or even most, of global ocean mixing but seek to show that they are one plausible mechanism of generating diapycnal mixing necessary to drive a meridional overturning circulation.

Although there is almost no understanding of the climate parameters that control tropical cyclone frequency (Henderson-Sellers et al. 1998), thermodynamic considerations have shown, in good agreement with observations, that the potential intensity of tropical cyclones increases with sea surface temperature (Emanuel 1987; Holland 1997; Tonkin et al. 2000). Furthermore, the observed cumulative distribution of tropical cyclone intensity implies that any increase in potential intensity would be accompanied by the same fractional increase in actual storm intensities (Emanuel 2000). It is plausible, then, that the climate state could affect the global average surface wind speeds and pressures associated with tropical cyclones.

A collection of studies suggests that the intense translating wind fields of hurricanes excite the ocean internal wave field to considerable depths with an energy distribution likely to transfer across the wave spectrum to the small dissipation scales needed for diapycnal mixing. The generation of near-inertial-frequency internal waves by hurricanes is supported both by observations (Brooks 1983; Shay and Elsberry 1987) and by modeling work (Geisler 1970; Price 1983). Niwa and Hibiya (1997) used a three-dimensional model to show that interactions between near-inertial waves in the wake of a hurricane excite internal waves with frequencies that are 2 and 3 times the local inertial frequency. The correlation of superinertial frequency waves with the times and locations of intense storms is supported by observations (D'Asaro et al. 1995; Niwa and Hibiya 1999). There is evidence that these low-vertical-mode superinertial-frequency waves supply energy to the internal wave spectrum that cascades down to small dissipation

scales, where it can result in shear instabilities and mixing (McComas and Muller 1981; Hibiya et al. 1996, 1998).

Nagasawa et al. (2000) modeled the distribution in the North Pacific Ocean of low-vertical-mode superinertial-frequency waves generated by tropical cyclones and storms and found that their vertically integrated energy is highest during autumn and winter around 10°–15°N in the western-central North Pacific. They note that microstructure measurements reporting diapycnal diffusivities of $10^{-5} \text{ m}^2 \text{ s}^{-1}$ (Gregg 1998) may have missed these locations and times of strong mixing. Although many of our experiments applied localized diffusivities that are considerably larger than is likely warranted by the mechanism of internal wave dissipation, they serve to examine the conceptual extreme in which almost all ocean mixing occurs on a highly transient, localized basis. The storm-induced modeled distribution of Nagasawa et al. is more zonally diffuse than our highly localized experiments, suggesting that a more realistic parameterization is likely some middle ground between our highly localized and boundary mixing scenarios.

An alternative to examining the detailed mechanisms of ocean mixing is to consider the net thermodynamic effects of this mixing. Emanuel (2001) estimated that global tropical cyclone activity induces a net ocean heating of $1.4 \pm 0.7 \text{ PW}$, which is a substantial fraction of the peak meridional heat flux of 2 PW estimated by Macdonald and Wunsch (1996). Although it could be argued that lateral fluxes redistribute this enthalpy locally, the results of this study and SM02 show that localized, transient mixing in the tropical thermocline does produce a global response.

The role of the ocean in net global heat transport depends crucially on diapycnal mixing, but existing parameterizations of mixing processes in models largely omit crucial feedbacks between mixing and the climate state. Wind-driven mixing, particularly that induced by tropical cyclones, could take part in such a feedback. The idealized experiments of this study serve as a feasibility test for one part of this feedback, showing that the MOC can be successfully driven by mixing with spatial and temporal distributions suggestive of tropical cyclones.

Acknowledgments. This manuscript benefited from the constructive comments of two anonymous reviewers. This work was supported in part through ONR (NOPP) ECCO Grant N00014-99-1-1050 and by the U.S. Department of Energy's Office of Biological and Environmental Research Grant DE-FG02-93ER61677. This is a contribution of the Consortium for Estimating the Circulation and Climate of the Ocean (ECCO) funded by the National Oceanographic Partnership Program.

REFERENCES

- Alford, M. H., 2001: Internal swell generation: The spatial distribution of energy flux from the wind to mixed layer near-inertial motions. *J. Phys. Oceanogr.*, **31**, 2359–2368.
- Brooks, D. A., 1983: The wake of Hurricane Allen in the western Gulf of Mexico. *J. Phys. Oceanogr.*, **13**, 117–129.
- D'Asaro, E. A., C. C. Eriksen, M. D. Levine, P. Niiler, C. A. Paulson, and P. Van Meurs, 1995: Upper-ocean inertial currents forced by a strong storm. Part I: Data and comparisons with linear theory. *J. Phys. Oceanogr.*, **25**, 2909–2936.
- Egbert, G. D., and R. D. Ray, 2001: Estimates of M_2 tidal energy dissipation from TOPEX/Poseidon altimeter data. *J. Geophys. Res.*, **106**, 22 475–22 502.
- Emanuel, K. A., 1987: The dependence of hurricane intensity on climate. *Nature*, **326**, 438–485.
- , 2000: A statistical analysis of tropical cyclone intensity. *Mon. Wea. Rev.*, **128**, 1139–1152.
- , 2001: Contribution of tropical cyclones to meridional heat transport by the oceans. *J. Geophys. Res.*, **106**, 14 771–14 781.
- Ferron, B., H. Mercier, K. Speer, A. Gargett, and K. Polzin, 1998: Mixing in the Romanche fracture zone. *J. Phys. Oceanogr.*, **28**, 1929–1945.
- Ganachaud, A., and C. Wunsch, 2000: Improved estimates of global ocean circulation, heat transport and mixing from hydrographic data. *Nature*, **408**, 453–457.
- Geisler, J. E., 1970: Linear theory of the response of a two layer ocean to a moving hurricane. *Geophys. Fluid Dyn.*, **1**, 249–272.
- Gent, P. R., and J. C. McWilliams, 1990: Isopycnal mixing in ocean circulation models. *J. Phys. Oceanogr.*, **20**, 150–155.
- Gregg, M. C., 1998: Estimation and geography of diapycnal mixing in the stratified ocean. *Physical Processes in Lakes and Oceans*, J. Imberger, Ed., Coastal and Estuarine Studies, Vol. 54, Amer. Geophys. Union, 305–338.
- Hasumi, H., and N. Sugimotohara, 1999: Effects of locally enhanced vertical diffusivity over rough bathymetry on the World Ocean circulation. *J. Geophys. Res.*, **104**, 23 367–23 374.
- Henderson-Sellers, A., and Coauthors, 1998: Tropical cyclones and global climate change: A post-IPCC assessment. *Bull. Amer. Meteor. Soc.*, **79**, 19–38.
- Hibiya, T., Y. Niwa, K. Nakajima, and N. Sugimotohara, 1996: Direct numerical simulation of the roll-off range of internal wave shear spectra in the ocean. *J. Geophys. Res.*, **101**, 14 123–14 129.
- , —, and K. Fujiwara, 1998: Numerical experiments of non-linear energy transfer within the oceanic internal wave spectrum. *J. Geophys. Res.*, **103**, 18 715–18 722.
- Holland, G. J., 1997: The maximum potential intensity of tropical cyclones. *J. Atmos. Sci.*, **54**, 2519–2541.
- Huang, R. X., 1999: Mixing and energetics of the oceanic thermohaline circulation. *J. Phys. Oceanogr.*, **29**, 727–746.
- Killworth, P. D., 1985: A two-level wind and buoyancy driven thermocline model. *J. Phys. Oceanogr.*, **15**, 1414–1432.
- Kunze, E., and T. B. Sanford, 1996: Abyssal mixing: Where it is not. *J. Phys. Oceanogr.*, **26**, 2286–2296.
- Legg, S., 2004: Internal tides generated on a corrugated continental slope. Part I: Cross-slope barotropic forcing. *J. Phys. Oceanogr.*, **34**, 156–173.
- Macdonald, A. M., and C. Wunsch, 1996: The global ocean circulation and heat flux. *Nature*, **382**, 436–439.
- Marotzke, J., 1990: Instabilities and multiple steady states of the thermohaline circulation. Ph.D. thesis, Ber. Inst. Meeresk. Kiel, 126 pp.
- , 1997: Boundary mixing and the dynamics of three-dimensional thermohaline circulations. *J. Phys. Oceanogr.*, **27**, 1713–1728.
- , and B. A. Klinger, 2000: The dynamics of equatorially asymmetric thermohaline circulations. *J. Phys. Oceanogr.*, **30**, 955–970.
- McComas, C. H., and P. Müller, 1981: The dynamic balance of internal waves. *J. Phys. Oceanogr.*, **11**, 970–986.
- McDougall, T. J., R. J. Greatbatch, and Y. Lu, 2002: On conservation equations in oceanography: How accurate are Boussinesq ocean models? *J. Phys. Oceanogr.*, **32**, 1574–1584.
- Moum, J. N., and T. R. Osborn, 1986: Mixing in the main thermocline. *J. Phys. Oceanogr.*, **16**, 1250–1259.
- Munk, W., 1966: Abyssal recipes. *Deep-Sea Res.*, **13**, 707–730.

- , and C. Wunsch, 1998: Abyssal recipes II: Energetics of tidal and wind mixing. *Deep-Sea Res.*, **45**, 1977–2010.
- Nagasawa, M., Y. Niwa, and T. Hibiya, 2000: Spatial and temporal distribution of the wind-induced internal wave energy available for deep water mixing in the North Pacific. *J. Geophys. Res.*, **105**, 13 933–13 943.
- Niwa, Y., and T. Hibiya, 1997: Nonlinear processes of energy transfer from traveling hurricanes to the deep ocean internal wave field. *J. Geophys. Res.*, **102**, 12 469–12 477.
- , and —, 1999: Response of the deep ocean internal wave field to traveling midlatitude storms as observed in long-term current measurements. *J. Geophys. Res.*, **104**, 10 981–10 989.
- Osborn, T. R., 1980: Estimates of the local rate of vertical diffusion from dissipation measurements. *J. Phys. Oceanogr.*, **10**, 83–89.
- Pacanowski, R. C., 1996: MOM 2.0 documentation, user's guide, and reference manual. NOAA/Geophysical Fluid Dynamics Laboratory Ocean Tech. Rep. 3.1, 350 pp. [Available from NOAA/GFDL, Princeton University, P.O. Box 308, Princeton, NJ 08542.]
- Polzin, K. L., J. M. Toole, J. R. Ledwell, and R. W. Schmitt, 1997: Spatial variability of turbulent mixing in the abyssal ocean. *Science*, **276**, 93–96.
- Price, J., 1983: Internal wave wake of a moving storm. Part I: Scales, energy budget and observations. *J. Phys. Oceanogr.*, **13**, 949–965.
- Redi, M. H., 1982: Oceanic isopycnal mixing by coordinate rotation. *J. Phys. Oceanogr.*, **12**, 1154–1158.
- Samelson, R. M., 1998: Large-scale circulation with locally enhanced vertical mixing. *J. Phys. Oceanogr.*, **28**, 712–726.
- Scott, J. R., 2000: The roles of mixing, geothermal heating, and surface buoyancy forcing in ocean meridional overturning dynamics. Ph.D. thesis, Massachusetts Institute of Technology, 128 pp.
- , and J. Marotzke, 2002: The location of diapycnal mixing and the meridional overturning circulation. *J. Phys. Oceanogr.*, **32**, 3578–3595.
- Shay, L. K., and R. L. Elsberry, 1987: Near-inertial ocean current response to Hurricane Frederic. *J. Phys. Oceanogr.*, **17**, 1249–1269.
- Tonkin, H., G. J. Holland, N. Holbrook, and A. Henderson-Sellers, 2000: An evaluation of thermodynamic estimates of climatological maximum potential tropical cyclone intensity. *Mon. Wea. Rev.*, **128**, 746–762.
- Toole, J. M., K. L. Polzin, and R. W. Schmitt, 1994: Estimates of diapycnal mixing in the abyssal ocean. *Science*, **264**, 1120–1123.
- , R. W. Schmitt, K. L. Polzin, and E. Kunze, 1997: Near-boundary mixing above the flanks of a midlatitude seamount. *J. Geophys. Res.*, **102**, 947–959.
- Winton, M., 1996: The role of horizontal boundaries in parameter sensitivity and decadal-scale variability of coarse-resolution ocean general circulation models. *J. Phys. Oceanogr.*, **26**, 289–304.
- Wunsch, C., 1998: The work done by the wind on the oceanic general circulation. *J. Phys. Oceanogr.*, **28**, 2332–2340.